RADIATION RESEARCH **161**, 732–738 (2004)
0033-7587/04 $15.00


TECHNICAL ADVANCE

# A Multi-port Low-Fluence Alpha-Particle Irradiator: Fabrication, Testing and Benchmark Radiobiological Studies

Prasad V. S. V. Neti, Sonia M. de Toledo, Venkatachalam Perumal, Edouard I. Azzam and Roger W. Howell[1]

*Department of Radiology, Division of Radiation Research, New Jersey Medical School, Newark, New Jersey 07103*

**Neti, P. V. S. V., de Toledo, S. M., Perumal, V., Azzam, E. I. and Howell, R. W. A Multi-port Low-Fluence Alpha-Particle Irradiator: Fabrication, Testing and Benchmark Radiobiological Studies. *Radiat. Res.* 161, 732–738 (2004).**

**A new multi-port irradiator, designed to facilitate the study of the effects of low fluences of α particles on monolayer cultures, has been developed. The irradiator consists of four individual planar $^{241}$Am α-particle sources that are housed inside a helium-filled Lucite chamber. Three of the radioactive sources consist of 20 MBq of $^{241}$Am dioxide foil. The fourth source, used to produce higher dose rates, has an activity of 500 MBq. The four sources are mounted on rotating turntables parallel to their respective 1.5-μm-thick Mylar exit windows. A stainless steel honeycomb collimator is placed between the four sources and their exit windows by a cantilever attachment to the platform of an orbital shaker that moves its table in an orbit of 2 cm. Each exit window is equipped with a beam delimiter to optimize the uniformity of the beam and with a high-precision electronic shutter. Opening and closing of the shutters is controlled with a high-precision timer. Custom-designed stainless steel Mylar-bottomed culture dishes are placed on an adapter on the shutter. The α particles that strike the cells have a mean energy of 2.9 MeV. The corresponding LET distribution of the particles has a mean value of 132 keV/μm. Clonogenic cell survival experiments with AG1522 human fibroblasts indicate that the RBE of the α particles compared to $^{137}$Cs γ rays is about 7.6 for this biological end point.** 

## INTRODUCTION

The adverse effects of exposure to α particles have been of considerable interest since Martland's early observations of health problems in radium dial painters at the Newark City Hospital[2] in Newark, NJ (*1, 2*). The mutagenic, carcinogenic and lethal effects of α particles have been well documented in cells that are traversed by these high-LET particles (*3–9*). The capacity of α particles to induce bystander effects has been demonstrated more recently (*10–13*). The term bystander effect is used to describe those effects that irradiated cells impart to neighboring unirradiated cells. The observation of bystander effects caused by α particles has led to a surge of interest in this phenomenon due to its potential importance in radiation protection and radiation therapy (*14–16*).

While a number of research groups have made substantial progress in elucidating the mechanisms of the bystander effect, there remains much to learn. However, there are presently only a limited number of the specialized α-particle irradiators that are required to carry out this work. Alpha-particle irradiators have been built around two basic designs: (1) microbeam and (2) broad beam. The term microbeam has been reserved for irradiators that have the capacity to deliver single α particles to specific intracellular targets (*17*). The advantage of these new and technologically advanced devices is not only their ability to deliver α particles one at a time, but also the accuracy with which they can deliver the particles (±3 μm). The principal disadvantages of these devices are that the cell throughput is slower (~10,000 cells per hour) than for broad-beam exposures and they require fluorescent dyes to be introduced into the cell prior to irradiation for targeting identification. Both of these drawbacks have the potential to have an impact on the biological end points being studied. Furthermore, access to the microbeams is limited because their high cost has restricted their numbers to only a few worldwide.

[1] Address for correspondence: Division of Radiation Research, Department of Radiology, MSB F-451, New Jersey Medical School, 185 South Orange Avenue, Newark, NJ 07103; e-mail: rhowell@umdnj.edu.

[2] Newark City Hospital, subsequently designated Martland Hospital, is now the Stanley S. Bergen, Jr. Administration Building of the University of Medicine & Dentistry of New Jersey, Newark, NJ. This building is adjacent to the Medical Science Building where our laboratories are located. Archives of Dr. Martland's work are held in the University Libraries Special Collections (http://www.umdnj.edu/librweb/speccoll/MARTLAND.htm).

Broad-beam α-particle irradiators have been available for quite some time. The principal advantage of these irradiators is high throughput and essentially no disturbance of the cultured cells prior to exposure. Specifically, large cell populations (millions of cells) can be exposed *rapidly* to low fluences of α particles so that a small fraction of the cells are hit. This facilitates observation of biological effects in a sizable population of bystander cells. Broad-beam systems are ideal for assaying end points that occur rapidly (e.g. gene expression), end points that require large numbers of cells, and highly sensitive end points that require minimization of stress caused by cell manipulations before, during and after exposure. The disadvantage of the broad-beam irradiator is that the bystander cells cannot be separated readily from the irradiated cells. However, cells can be grown and irradiated on radiation-sensitive films that enable correlation of *in situ* responses with cells that are hit (*18*). These irradiators have been built around two basic platforms, accelerators (*19, 20*) and radioactive sources (*21–26*). Accelerator-based machines are expensive to maintain and relatively inaccessible. Alpha-particle irradiators that use radioactive sources are also relatively scarce, in part because of policies that discourage the use of such sources. This is unfortunate considering the heightened interest in the field. Therefore, there is a need to develop simple and inexpensive α-particle irradiators that are based on readily available technology. The present work describes and characterizes an α-particle irradiator that fulfills these requirements.

## MATERIALS AND METHODS

### *Alpha-Particle Sources*

The radionuclide $^{241}$Am is used as the source of α particles. This radionuclide was chosen because of its long physical half-life (432.2 years) and widespread availability owing to its use in smoke detection systems. The principal α-particle radiations emitted are 5.485, 5.443 and 5.388 MeV with corresponding yields per decay of 0.845, 0.13 and 0.016, respectively (*27*). The principal photon emitted is the 59.5 keV γ ray with a yield of 0.359 per decay (*27*). Four $^{241}$Am dioxide foils are mounted in the irradiator (Model A-001, NRD Incorporated, Grand Island, NY). Three of the sources contain 20 MBq (0.34 MBq/cm$^2$) while the fourth source, used to produce higher dose rates, contains 500 MBq (8.6 MBq/cm$^2$). The material is a laminated metallic foil of silver, gold and americium dioxide. The foil is comprised of six successive layers: 0.5 μm gold, 1 μm gold, 0.5 μm $^{241}$Am and gold, 0.75 μm gold, 10–23 μm silver, and flash plating for identification. The first two layers of gold comprise a protective layer through which the α particles travel *en route* to the cells.

### *Alpha-Particle Irradiator*

The basic design of Metting *et al.* (*25*) was adopted and further developed. The major changes are an electronic shutter system, multiple exit windows to facilitate simultaneous irradiation of replicate samples and/or different fluences, and use of inexpensive and readily available $^{241}$Am sources as opposed to a $^{238}$Pu source. The present design consists of several major components: the $^{241}$Am sources (described above), source rotation system, collimator system, beam delimeter and exit window, electronic shutter system, and Mylar-bottomed cell culture dish. The $^{241}$Am sources, source rotation system, collimator system, beam delimeter, and α-particle exit window are all mounted within a sealed 1.2-cm-thick Lucite chamber (Grewe Plastics, Newark, NJ). To minimize attenuation of the α particles, helium is passed through a DuraDRY 814-BX filter (Parker, Haverhill, MA) and injected into the chamber (500 cm$^3$/min, Cole Parmer 65-mm flowmeter, Vernon Hills, IL) overnight through two flanged NPT fittings located at the top of the rear wall of the chamber. Two flanged NPT exit ports are connected to a Gelman Model 1119 47-mm in-line filter holder (Gelman Sciences Inc., Ann Arbor, MI) loaded with a Gelman Type AE glass fiber filter. The removable filter facilitates checking for contamination arising from failure of the $^{241}$Am source seals. A photograph of the complete system can be viewed at http://www.umdnj.edu/radreweb/facilities/alpha_particle.htm.

### *Source Rotation System*

The $^{241}$Am foils are mounted with specialty tape Model FT A (Avery Dennison, Painesville, OH) onto 7.6 × 7.6-cm$^2$ aluminum plates that are 0.32 cm thick. An aluminum cylindrical sleeve with locking screws was used to attach each plate to a Hansen Model 116-42612-2 DC gearbox motor (Hansen Corp., Princeton, IN). The motors, powered by a 12 V d.c. regulated power supply, were used to rotate the α-particle sources at 88 rpm to ensure maximum beam uniformity. The source rotation assembly was mounted vertically on a custom Lucite bracket. The source rotation system holds the surface of the sources 4.5 cm from the exit window.

### *Collimator System*

To reduce the maximum angle of incidence upon the growth surface of the culture dishes, a large collimator is placed between the $^{241}$Am foils and the four Mylar exit windows. The collimator is designed with a 46 × 34 × 0.66-cm sheet of Model no. 8728 stainless steel honeycomb (Innovent, Peabody, MA) made with foil of thickness 0.00508 cm. The hexagonal cells are 0.3175 cm across. The collimator is suspended above the $^{241}$Am foils by a bracket made of aluminum and Lucite that is mounted on capstans to a Barnstead|Thermolyne Model M50825 Rotomix Variable Speed Rotator (Dubuque, IA). The Rotomix oscillates the collimator in a plane parallel to the $^{241}$Am sources at a rate of 150 orbits per minute with an orbit diameter of 2 cm to prevent masking of the cells by the collimator.

### *Beam Delimeter and Exit Window*

The design of Metting *et al.* (*25*) was adopted for the beam delimeter and exit window. They showed that use of a tapered beam delimeter substantially improved the uniformity of the beam, particularly at the edges of the growth surface. The beam delimeter was machined from 1.2-cm-thick Lucite and tapered outward toward the source at an angle of 22° (Grewe Plastics). The circular opening at the top of the beam delimeter, which defines the beam, has a diameter of 4.5 cm. A 1.5-μm-thick piece of Mylar was gently stretched and affixed (Avery Dennison FT A) to the top of the beam delimeter to serve as the exit window. Figure 1 shows a scale drawing of the irradiator with source rotation system, collimator system, and beam delimeter.

### *Exposure Shutters and Timing System*

Exposure times are controlled by Copal Model DC-392 electromechanical shutters (Nidec Copal Corporation, Tokyo). These shutters have apertures 80 mm in diameter and accommodate shutter speeds of 0.125 s or longer. Shutter speeds of ~1 s or more are recommended to ensure uniform exposure of the Mylar-bottomed dish. The shutter operation is controlled by a Logotron® LGT 12C DC control and timing relay powered by a Model EN50178 power supply with 1 A maximum output (Entrelec International, Irving, TX). Adapters that mount on top of the Copal shutters to hold the stainless steel culture dishes were manufactured by Grewe Plastics.

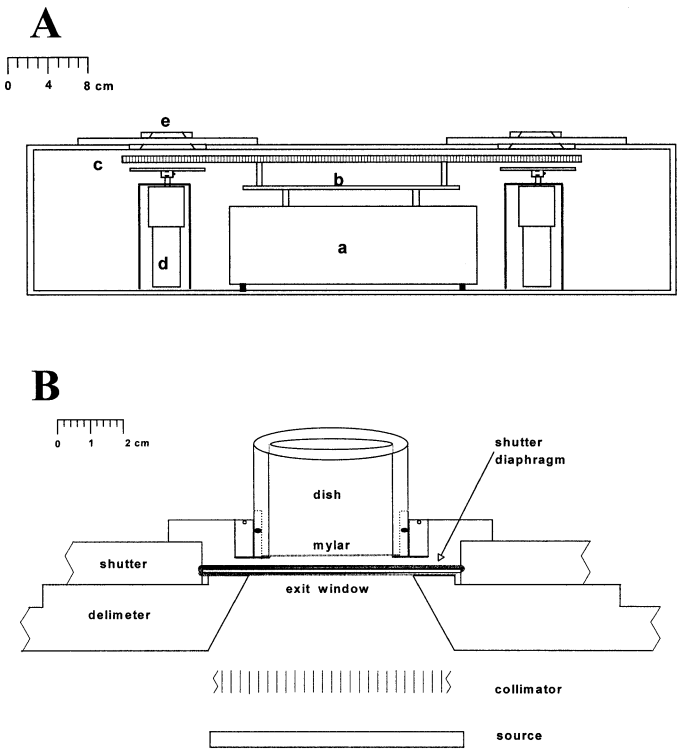


**FIG. 1.** Panel A: Scale drawing of the front view of the irradiator featuring some of the major components: (a) orbital shaker base, (b) orbital shaker platform, (c) stainless steel honeycomb collimator, (d) source rotation assembly, and (e) beam delimeter with 1.5-μm-thick Mylar exit window. Panel B: Detailed enlargement of the irradiator components involved in producing the α-particle beam. The scales for A and B are denoted in the upper left corner of each panel.

*Cell Culture Dishes*

Cell culture dish assemblies were machined[3] from TYPE 304 stainless steel pipe (schedule 80 and 40) in the same manner as those of Metting *et al.* (*25*). As shown in Fig. 2 in ref. (*25*), the assemblies consist of a −030 Viton rubber O-ring (Greene Rubber Co., Woburn, MA) and two cylindrical stainless steel parts that interlock in such a manner as to stretch a 1.5-μm-thick Mylar film into a circular 36-mm-diameter growing surface.

*Alpha-Particle Energy Spectrum*

The energy spectrum of the α-particle beam was measured using a Canberra (Meridien, CT) CAM300 passive implanted planar silicon (PIPS) detector. This detector has an active area of 300 mm$^2$. The CAM300 PIPS intrinsic detection efficiency for a collimated beam of α particles is 100% over the energy range used in this work. Conventional nucleonics (Canberra) and a multichannel analyzer were used to obtain energy spectra. The detector was calibrated for energy response in a vacuum using a Model S94-4 planar $^{239}$Pu calibration standard (427,445 cpm/2π) from Eberline (Albuquerque, NM). The $^{239}$Pu principally emits 5.105, 5.143 and 5.156 MeV α particles with corresponding yields per decay of 0.106, 0.151 and 0.732 (*27*). The standard was maintained in a vacuum at a distance of 4.5 cm from the PIPS detector. The 5.105, 5.143 and 5.156 MeV α particles were not resolved, and hence a single peak was obtained with centroid at channel 3297.9 with FWHM of 86.5 channels. This corresponds to a mean energy of 5.14 MeV with FWHM of 0.13 MeV (Fig. 2). After the calibration was complete, the spectrum emitted by one of the 20 MBq $^{241}$Am sources was also measured under vacuum using the same geometry except that the beam was collimated with a small hole to reduce the α-particle flux. The $^{241}$Am α-particle spectrum, shown in Fig. 2, had a centroid at 4.76 MeV with FWHM of 0.47 MeV. The spectrum matched that provided by the manufacturer. Once calibrated, the detector was positioned on the Mylar growing surface of a stainless steel culture dish and radiation spectra were acquired for each source. Figure 3A shows a representative energy spectrum for one of the sources.

[3] Machining performed by Ashley Webb, Greenfield, MA.

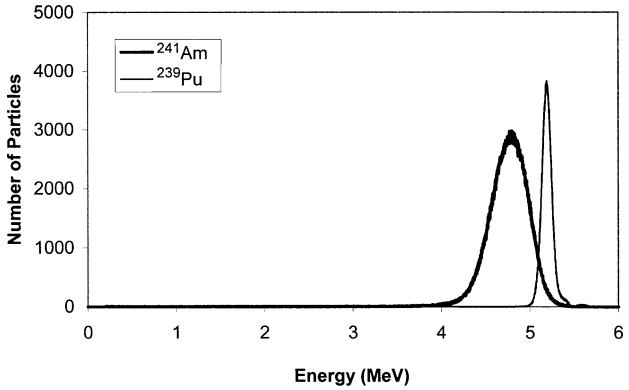


**FIG. 2.** Alpha-particle energy spectrum acquired for a 20 MBq $^{241}$Am source and a planar $^{239}$Pu standard maintained in a vacuum. The mean energy of the $^{239}$Pu α particles is 5.14 MeV with a FWHM of 0.13 MeV. The corresponding values for $^{241}$Am are 4.76 and 0.47 MeV, respectively.

*LET Spectrum*

To determine the LET spectrum of the α particles incident on the cells growing in the Mylar-bottomed culture dishes, the LET values corresponding to the energies associated with each of the 4096 channels were calculated by interpolating the tables for liquid water in ICRU Report 49 (*28*). The tables in Report 49 indicate that the LET of α particles in water has a maximum of about 227 keV/μm at 0.7 MeV. Thus α particles corresponding to energies on either side of the peak may have the same LET. For example, both 0.2 MeV and 2.0 MeV α particles have an LET of about 160 keV/μm. Accordingly, the LET spectrum was obtained by creating bins 5 keV/μm wide (e.g. 80–85 keV/μm, 85–90 keV/μm, etc.) and then summing counts into the appropriate bins.

*Uniformity of the Alpha-Particle Beam*

Beam uniformity was assessed with CR-39 plastic obtained from Track Analysis Systems, Ltd. (Bristol, UK). The plastic was precut by the manufacturer into circular pieces that fit into the cell culture dish adapters. Exposure times of 4 s were used that were commensurate with typical irradiation times used in bystander effect experiments. The plastic was etched according to the manufacturer's instructions. CR-39 plastic is sensitive to α particles and is not sensitive to X rays and γ rays. Thus only the α particles emitted by $^{241}$Am were detected. The processed plastic was viewed at 150× magnification with an Olympus IX70 inverted microscope (Tokyo, Japan) equipped with a green filter, digital camera, and video monitor. A hemocytometer was placed in the viewing field and tape was used to define a region on the video screen corresponding to a ⅛-mm$^2$ region of the hemocytometer. The pits created by the etching process were scored at 40 locations along the entire diameter of the CR-39 plastic corresponding to the diameter of the Mylar growing surface.

*Benchmark Cell Survival Curve for AG1522 Human Fibroblasts*

AG1522 normal human diploid fibroblasts at passage 10–11 were used (Coriell Institute for Medical Research, Camden, NJ). The cells were maintained in Eagle's minimum essential medium (Sigma, St. Louis, MO) supplemented with 12.5% heat-inactivated (56°C, 30 min) fetal calf serum

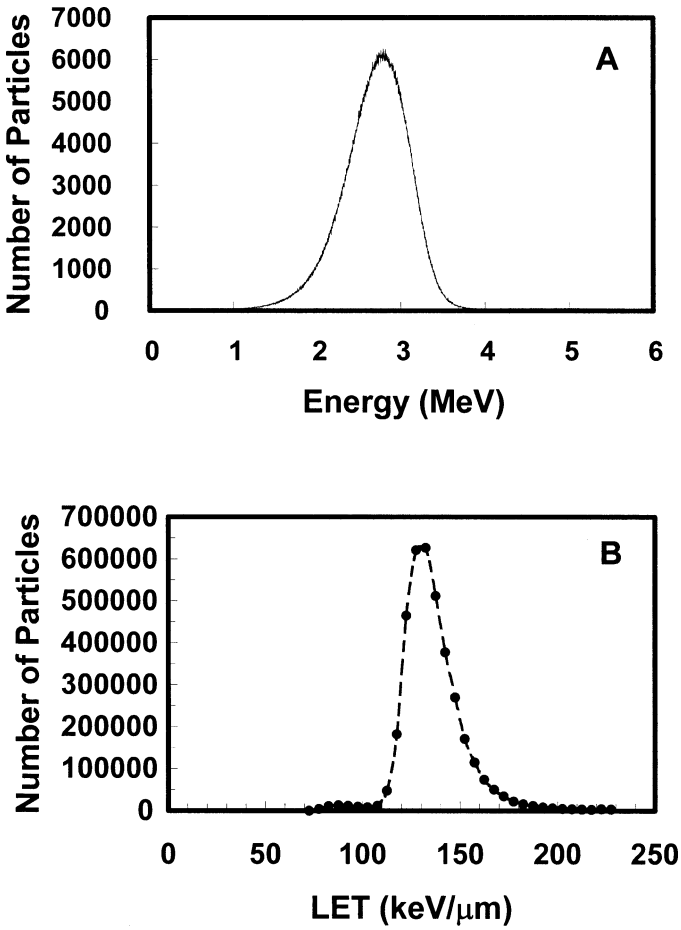


**FIG. 3.** Alpha-particle spectrum obtained for Source 2 of the α-particle irradiator. Panel A: Energy spectrum (4096 channels). Panel B: LET spectrum (circles designate the sum of events in bins of width 5 keV/μm). The irradiator chamber was flushed with helium overnight and the detector placed directly against the growth surface of the Mylar-bottomed cell culture dish.

and 0.025 mg/ml gentamicin sulfate. The cells were incubated at 37°C in a humidified atmosphere of 5% $CO_2$ in air. Cells destined for α-particle irradiation were suspended in growth medium and seeded at a density of $10^5$ cells per dish in stainless steel Mylar-bottomed dishes. They were fed with growth medium on days 5, 7 and 9, and experiments were started 48 h after the last feeding. At that time, the culture was confluent and contained about $10^6$ cells (98% in $G_0/G_1$ phase of the cell cycle). Cell dose–response survival curves were obtained by irradiating the cultures with graded mean doses of α particles. For comparison, additional cells grown to similar confluence in standard 60-mm culture dishes (Corning, Corning, NY) were irradiated with $^{137}$Cs γ rays delivered with a J. L. Shepherd Mark I Irradiator (J. L. Shepherd & Associates, San Fernando, CA) at a dose rate of 90 cGy/min. The irradiated cultures were washed with phosphate-buffered saline (PBS), trypsinized, resuspended in growth medium, serially diluted, and seeded into Falcon 100-mm culture dishes in sufficient numbers to form about 150 colonies. After 2 weeks, the resulting colonies were washed with PBS, fixed with ethanol, and stained with crystal violet. Colonies (>50 cells) were scored under low magnification with an Olympus dissecting microscope. Surviving fractions normalized to controls were determined.

## RESULTS

### *Energy and LET Spectra*

Figure 3A shows the α-particle energy spectrum recorded on the growth surface of the Mylar-bottomed cell culture dish for one of the 20 MBq sources. The centroid of the peak is 2.9 MeV. The corresponding LET spectrum is shown in Fig. 3B. The LET spectrum ranges from about 70 to 200 keV/μm with a mean value of 132 keV/μm. Similar spectra were recorded for the remaining 20 MBq sources.

### *Alpha-Particle Fluence and Uniformity of the Beam*

The α-particle fluence was calculated by integrating the counts from 0.2 MeV to 6.0 MeV during a 200-s acquisition and dividing by the active area of the PIPS detector (300 $mm^2$). These data are shown in the first row of Table 1. The very small number of counts corresponding to energies below 0.2 MeV was not taken into account because the photopeak corresponding to the $^{241}$Am 60 keV γ ray prevented an accurate determination of them.

The uniformity of the α-particle beam was also assessed with CR-39 plastic. Pits were counted in 40 fields of 125,000 $\mu m^2$ each across the diameter of the dish. The mean number of pits per field was 26.1 ± 5.0, 26.2 ± 4.7 and 27.0 ± 5.2 for sources 1, 2 and 3, respectively, for a 4-s irradiation time. The indicated standard deviations of the mean (SD) are close to their expected values for a Poisson distribution, the square roots of the means. These measurements were also used to calculate the fluence. These values are shown in the second row of Table 1.

### *Benchmark Cell Survival Curve for AG1522 Human Fibroblasts*

Figure 4 shows the benchmark survival curve for confluent density-inhibited AG1522 cells irradiated with α particles using the irradiator described in this report. The dose–response curve for $^{137}$Cs γ rays is shown for comparison. A least-squares fit of the α-particle data to an exponential function gave SF(α particles) = exp(–0.0327 *D*), where *D*

**TABLE 1**
**Fluence [tracks/($\mu m^2$ min)]**

| Measurement method | Source 1 | Source 2 | Source 3 |
|---|---|---|---|
| CAM300 PIPS[a] | 0.0038 ± 0.0001 | 0.0037 ± 0.0001 | 0.0034 ± 0.0001 |
| CR-39[b] | 0.0031 ± 0.0006 | 0.0031 ± 0.0006 | 0.0032 ± 0.0006 |

[a] Estimated error for CAM300 PIPS measurements is based on reproducibility of measurement.
[b] Estimated error for CR-39 measurements is the SDM of tracks counted in 40 fields.

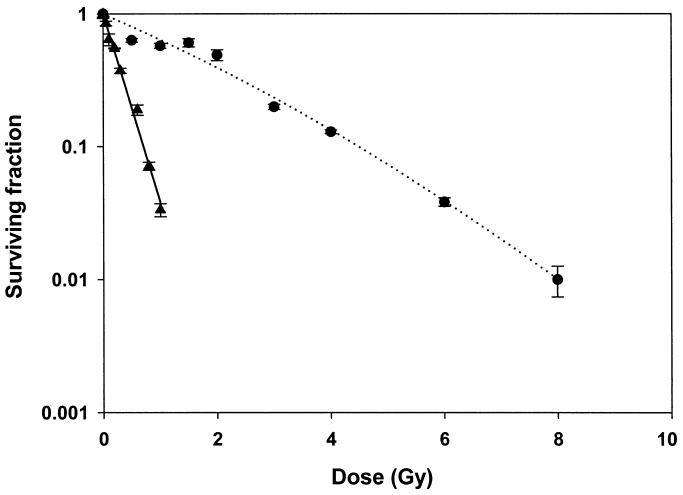


**FIG. 4.** Clonogenic survival of confluent AG1522 human fibroblasts exposed to α particles (triangles) or γ rays (circles). The respective responses with and without a shoulder are characteristic for these radiation types.

is the mean absorbed dose (cGy) to the cell layer. A least-squares fit of the γ-ray data to the linear-quadratic model gave SF(γ rays) = $\exp(-4.3 \times 10^{-3}\, D - 1.8 \times 10^{-6}\, D^2)$. The corresponding doses required to achieve 37% survival ($D_{37}$) are 30.6 ± 1.3 cGy and 2.33 ± 0.49 Gy for α particles and γ rays, respectively. The α-particle response is very similar to the value of 35 cGy obtained by Raju *et al.* (*7*) with the same cell line. The relative biological effectiveness (RBE) of the α particles compared to $^{137}$Cs γ rays is about 7.6 ± 1.6 for AG1522 cells.

## DISCUSSION

Ideally, experiments with low-fluence α-particle beams should be carried out with monoenergetic α particles that travel perpendicular to the plane of the surface upon which the cells are growing. While the trajectory of the particles is controlled with a collimator, attainment of a monoenergetic beam with a simple low-cost design is difficult due to technical constraints. The three principal α particles emitted by $^{241}$Am are, from a radiobiological standpoint, essentially monoenergetic (5.485, 5.443 and 5.388 MeV). However, absorbing materials that are placed between the $^{241}$Am and the target cells cause attenuation of the beam and consequent broadening of the energy spectrum. In the present irradiator, there are several layers of attenuating material between the radioactive source and the cells: gold foil layered over the $^{241}$Am, helium gas between the foil and the exit window, the Mylar exit window, air between the Mylar window and the Mylar bottom of the culture dish, and finally the Mylar bottom of the dish. While each layer serves a necessary purpose, each layer also contributes to broadening of the energy spectrum. Figure 2 shows the broadening due to the gold foil that is layered over the $^{241}$Am. The increased broadening of the $^{241}$Am α-particle energy spectrum shown in Fig. 3A is due to the remaining layers of attenuating material. Some of the broadening could be eliminated if the helium was replaced with a vacuum and the Mylar bottom was used as both a growth surface and the exit window, thereby eliminating the air gap. This approach was used by Barendsen and Beusker (*21*) in one of their α-particle irradiator designs, although beam uniformity was not optimal in their design. In any case, the need for a very thin, large-diameter exit window imposes constraints on the use of a vacuum. For a helium-filled design, use of the Mylar growth surface as the exit window would introduce air into the chamber each time the dish is changed. This would cause fluctuations in the energy spectrum for different runs. While the present design produces a broad energy spectrum, it delivers a broad and uniform beam of α particles on the cell growth surface with a highly reproducible fluence and energy spectrum.

Figure 3B shows the LET distribution of the α particles in the cells assuming that they are composed of water. The LET ranges from about 70 to 200 keV/μm with a mean value of 132 keV/μm. Thus, based on past studies on the dependence of RBE on LET (*29*), one can anticipate that the RBE of the α particles is likely to range from about 5 to 8 for survival of mammalian cells. This expectation is borne out by the data in Fig. 4. For AG1522 cells, the mean RBE of the α particles emitted by the present irradiator compared to $^{137}$Cs γ rays is 7.6 ± 1.6 at 37% survival. This is somewhat higher than the data of Raju *et al.* (*7*) that

**TABLE 2**
**Dosimetry Parameters for Source 2[a]**

| Dose (cGy) | Exposure time (s)[b] | $f(0)$ | $f(1)$ | $f(2)$ | $f(3)$ | $f(4)$ | $f(>4)$ |
|---|---|---|---|---|---|---|---|
| 0.5 | 3.75 | 0.967 | 0.0322 | 0.000537 | $5.97 \times 10^{-6}$ | $4.98 \times 10^{-8}$ | |
| 1 | 7.5 | 0.936 | 0.0623 | 0.00208 | $4.62 \times 10^{-5}$ | $7.7 \times 10^{-7}$ | |
| 2 | 15 | 0.875 | 0.117 | 0.00778 | 0.000346 | $1.15 \times 10^{-5}$ | |
| 5 | 37 | 0.717 | 0.239 | 0.0398 | 0.00442 | 0.000369 | |
| 10 | 75 | 0.513 | 0.342 | 0.114 | 0.0254 | 0.00423 | 0.00137 |
| 20 | 150 | 0.264 | 0.351 | 0.234 | 0.104 | 0.0347 | 0.0123 |
| 50 | 375 | 0.136 | 0.119 | 0.198 | 0.220 | 0.184 | 0.143 |

[a] $f(i)$ denotes fraction of cells receiving $i$ traversals.
[b] Average dose rate at Mylar growth surface is 0.080 Gy/min = 0.133 cGy/s.

yield an RBE at 37% survival of 4.9 compared to $^{60}$Co $\gamma$ rays.

Using the terminology and methods of Charlton and Sephton (*30*), the absorbed dose received by a single traversal through the cell nucleus and the percentage of cells traversed can be calculated. Briefly, the dose per traversal $d$ to the thin disk-shaped cell nucleus of the AG1522 cell is given by $d = (0.16)(\text{LET})/A$, where $A$ is the cross-sectional area of the cell nucleus. The units for $d$, LET and $A$ are Gy, keV/$\mu$m and $\mu$m$^2$, respectively. This formula is valid only in cases where the ranges of the $\delta$ rays are small compared to the nuclear diameter (maximum range of the $\delta$ rays produced by a 3.65 MeV $\alpha$ particle is about 0.1 $\mu$m (*31*). Raju *et al.* (*7*) reported a value of $A = 144$ $\mu$m$^2$ for AG1522 cells. With a mean LET of 132 keV/$\mu$m, the calculated absorbed dose to the cell nucleus of an AG1522 cell from a single $\alpha$-particle traversal is therefore 0.15 Gy. While this is a mean value for a single traversal, the value for any given traversal would vary depending on the particulars of the particle and cell, namely LET and cross-sectional area of cell nucleus. The cellular parameters vary regardless of the beam characteristics (monoenergetic or polyenergetic); therefore, the dose for a single traversal varies from cell to cell regardless of whether a broad beam or microbeam is used to deliver the particle. The mean dose $D$ to the cell population is given by $D = F\,A\,d$, where $F$ is the fluence (tracks/$\mu$m$^2$) (*30*). Given the fluences of 0.0038, 0.0037 and 0.0034 tracks/($\mu$m$^2$ min) obtained for Sources 1, 2 and 3 with the PIPS detector, respectively, the mean absorbed dose rates to a monolayer would be 0.082, 0.080 and 0.073 Gy/min, respectively. Only a small fraction of the cells are traversed in a culture exposed to low average doses of $\alpha$ particles. According to Charlton and Sephton (*30*), the fraction of cells $f$ receiving exactly $i$ traversals is $f = (D/d)^i \exp(-D/d)/(i!)$. Therefore, for confluent cultures of AG1522 cells, the fractions of cells receiving a single hit are 0.019, 0.038 and 0.062 at mean doses of 0.3, 0.6 and 1 cGy. Table 2 gives the exposure time required to deliver various mean doses to the cell population along with the fraction of AG1522 cell nuclei that receive various numbers of traversals.

The absorbed dose calculations described above use the fluences measured by the PIPS detector. It is interesting to compare these fluences (Table 1, row 1) with those obtained with the CR-39 plastic (Table 1, row 2). The fluences obtained with the CR-39 plastic are lower than those obtained with the PIPS detector, although they are within the experimental uncertainties of the measurements. The fluences obtained with the PIPS detector have a much higher degree of accuracy and precision than the CR-39 measurements and are therefore taken as the definitive values.

This irradiator is particularly useful for studies on the bystander response where a small fraction of the cells' nuclei in an exposed culture are actually traversed by an $\alpha$-particle track. An understanding of the mechanisms underlying low-fluence exposure could have a direct impact on radiation risk estimates because a large component of the background exposure dose received by the general public from all sources of ionizing radiation arises from $\alpha$ particles emitted by radon and its progeny. The U.S. National Academy of Sciences estimates that 10 to 14% of all lung cancer deaths are linked to radon gas in the environment (*32*). Low-fluence studies can also have a significant implication in radiotherapy whereby irradiated cells can modulate signaling pathways in neighboring malignant or normal cells.

## ACKNOWLEDGMENTS

This work was supported in part by the New Jersey Commission on Cancer Research Grant No. 02-1081-CCR-S2 (EIA) and USPHS Grant Nos. CA83838 (RWH) and CA92262 (EIA).

Received: November 19, 2002; accepted: January 15, 2004

## REFERENCES

1. H. S. Martland, Microscopic changes of certain anemias due to radioactivity. *Arch. Pathol. Lab. Med.* **2**, 465–472 (1926).
2. H. S. Martland, The occurrence of malignancy in radioactive persons. *Am. J. Cancer* **15**, 2435–2516 (1931).
3. G. W. Barendsen, Dose–survival curves of human cells in tissue culture irradiated with alpha-, beta-, 20-kV. X- and 200-kV. X-radiation. *Nature* **193**, 1153–1155 (1962).
4. National Research Council, Committee on the Biological Effects of Ionizing Radiation, *Health Risks of Radon and Other Internally Deposited Alpha Emitters* (*BEIR IV*). National Academy Press, Washington, DC, 1988.
5. R. D. Lloyd, G. N. Taylor, W. Angus, S. C. Miller and B. B. Boecker, Skeletal malignancies among beagles injected with $^{241}$Am. *Health Phys.* **66**, 172–177 (1994).
6. R. D. Lloyd, G. N. Taylor, W. Angus and S. C. Miller, Soft tissue tumors in beagles injected with $^{241}$Am citrate. *Health Phys.* **68**, 225–233 (1995).
7. M. R. Raju, Y. Eisen, S. Carpenter and W. C. Inkret, Radiobiology of $\alpha$ particles. III. Cell inactivation by $\alpha$-particle traversals of the cell nucleus. *Radiat. Res.* **128**, 204–209 (1991).
8. R. W. Howell, S. M. Goddu, V. R. Narra, D. R. Fisher, R. E. Schenter and D. V. Rao, Radiotoxicity of gadolinium-148 and radium-223 in mouse testes: Relative biological effectiveness of alpha-particle emitters *in vivo*. *Radiat. Res.* **147**, 342–348 (1997).
9. D. V. Rao, V. R. Narra, G. F. Govelitz, V. K. Lanka, R. W. Howell and K. S. R. Sastry, *In vivo* effects of 5.3 MeV alpha particles from Po-210 in mouse testes: Comparison with internal Auger emitters. *Radiat. Prot. Dosim.* **31**, 329–332 (1990).
10. H. Nagasawa and J. B. Little, Induction of sister chromatid exchanges by extremely low doses of alpha-particles. *Cancer Res.* **52**, 6394–6396 (1992).
11. A. Deshpande, E. H. Goodwin, S. M. Bailey, B. L. Marrone and B. E. Lehnert, Alpha-particle-induced sister chromatid exchange in normal human lung fibroblasts—Evidence for an extranuclear target. *Radiat. Res.* **145**, 260–267 (1996).
12. E. I. Azzam, S. M. de Toledo, T. Gooding and J. B. Little, Intercellular communication is involved in the bystander regulation of gene expression in human cells exposed to very low fluences of alpha particles. *Radiat. Res.* **150**, 497–504 (1998).
13. E. I. Azzam, S. M. de Toledo and J. B. Little, Oxidative metabolism, gap junctions and the ionizing radiation-induced bystander effect. *Oncogene* **22**, 7050–7057 (2003).
14. J. B. Little, Radiation carcinogenesis. *Carcinogenesis* **21**, 394–404 (2000).
15. H. Zhou, G. Randers-Pehrson, C. A. Waldren, D. Vannais, E. J. Hall

and T. K. Hei, Induction of a bystander mutagenic effect of alpha particles in mammalian cells. *Proc. Natl. Acad. Sci. USA* **97**, 2099–2104 (2000).

16. E. I. Azzam, S. M. de Toledo and J. B. Little, Direct evidence for the participation of gap-junction mediated intercellular communication in the transmission of damage signals from alpha-particle irradiated to non-irradiated cells. *Proc. Natl. Acad. Sci. USA* **98**, 473–478 (2001).
17. G. Randers-Pehrson, C. R. Geard, G. Johnson, C. D. Elliston and D. J. Brenner, The Columbia University single-ion microbeam. *Radiat. Res.* **156**, 210–214 (2001).
18. C. Søyland, S. P. Hassfjell and H. B. Steen, A new alpha-particle irradiator with absolute dosimetric determination. *Radiat. Res.* **153**, 9–15 (2000).
19. G. W. Barendsen, M. D. Walter, J. F. Fowler and D. K. Bewley, Effects of different ionizing radiations on human cells in tissue culture III. Experiments with cyclotron-accelerated alpha-particles and deuterons. *Radiat. Res.* **18**, 106–119 (1963).
20. B. Rydberg, L. Heilbronn, W. R. Holley, M. Lobrich, C. Zeitlin, A. Chatterjee and P. K. Cooper, Spatial distribution and yield of DNA double-strand breaks induced by 3–7 MeV helium ions in human fibroblasts. *Radiat. Res.* **158**, 32–42 (2002).
21. G. W. Barendsen and T. L. J. Beusker, Effects of different ionizing radiations on human cells in tissue culture I. Irradiation techniques and dosimetry. *Radiat. Res.* **13**, 832–840 (1960).
22. R. Datta, A. Cole and S. Robinson, Use of track-end alpha particles from $^{241}$Am to study radiosensitive sites in CHO cells. *Radiat. Res.* **65**, 139–151 (1976).
23. C. Lücke-Huhle, W. Comper, L. Hieber and M. Pech, Comparative study of $G_2$ delay and survival after $^{241}$Am-$\alpha$ and $^{60}$Co-gamma-irradiation. *Radiat. Environ. Biophys.* **20**, 171–185 (1982).
24. D. T. Goodhead, D. A. Bance, A. Stretch and R. E. Wilkinson, A versatile plutonium-238 irradiator for radiobiological studies with alpha-particles. *Int. J. Radiat. Biol.* **59**, 195–210 (1991).
25. N. F. Metting, A. M. Koehler, H. Nagasawa, J. M. Nelson and J. B. Little, Design of a benchtop alpha particle irradiator. *Health Phys.* **68**, 710–715 (1995).
26. W. C. Inkret, Y. Eisen, W. F. Harvey, A. M. Koehler and M. R. Raju, Radiobiology of alpha particles. I. Exposure system and dosimetry. *Radiat. Res.* **123**, 304–310 (1990).
27. E. Browne and R. B. Firestone, *Table of Radioactive Isotopes.* Wiley, New York, 1986.
28. ICRU, *Stopping Powers and Ranges for Protons and Alpha Particles.* Report 49, International Commission on Radiation Units and Measurements, Bethesda, MD, 1993.
29. G. W. Barendsen, Impairment of the proliferative capacity of human cells in cultures by $\alpha$ particles of differing linear energy transfer. *Int. J. Radiat. Biol.* **8**, 453–466 (1964).
30. D. E. Charlton and R. Sephton, A relationship between microdosimetric spectra and cell survival for high-LET irradiation. *Int. J. Radiat. Biol.* **59**, 447–457 (1991).
31. R. N. Hamm, J. E. Turner, R. H. Ritchie and H. A. Wright, Calculation of heavy-ion tracks in liquid water. *Radiat. Res.* **104** (Suppl.), S20–S26 (1985).
32. National Research Council, Committee on the Biological Effects of Ionizing Radiation, *Health Effects of Exposure to Radon (BEIR VI).* National Academy Press, Washington, DC, 1999.